ORIGINAL ARTICLE

Green synthesis of silver nanoparticles using *Moringa oleifera* and its efficacy against gram-negative bacteria targeting quorum sensing and biofilms

Zarrin Haris[1] · Iqbal Ahmad[1]

Abstract

Gram-negative pathogenic bacteria are the leading cause of high morbidity and mortality in humans globally. The majority of such pathogens has gained the status of multidrug resistance and requires the development of new anti-pathogenic agent. *Moringa oleifera* is a widely distributed and quickly proliferating medicinal plant, making it an easy source for extracting bioactive components. It is rich in bioactive compounds which can act as stabilizing and reducing agents during the synthesis of silver nanoparticles. It is well-recognized for its several medical benefits, including antibacterial action. As a result, it is an excellent option for synthesizing AgNPs with improved antibacterial characteristics. Considering the above properties, less explored *Moringa oleifera* was used for the green synthesis of nanoparticles. Targeting biofilms and virulence factors of Gram-negative bacteria by green synthesized metal nanoparticles is an alternative approach to combat antimicrobial resistance. Silver nanoparticles (MO-AgNPs) synthesized using *Moringa oleifera* leaf (MOL) extract were characterized using Ultraviolet–visible spectroscopy (UV–vis spectroscopy), Fourier-transform infrared spectroscopy (FTIR), Scanning electron microscopy-energy dispersive X-ray analysis (SEM–EDX), Transmission Electron Microscopy (TEM), and X-Ray Diffraction analysis (XRD). The absorption spectra of silver nanoparticles showed a band of absorption near 440 nm, associated with spherical silver nanoparticles. At sub-minimum inhibitory concentrations (sub-MICs), the MO-AgNPs inhibit the Quorum Sensing-mediated virulence factors and biofilm formation against three Gram-negative bacteria (*Escherichia fergusonii, Serratia marcescens, and Chromobacterium violaceum*). QS-mediated virulence factors in test bacteria were reduced by 80.67% (violacein), prodigiosin production (77.45%), exoprotease activity (76.02%), and swarming motility (86.5%). MO-AgNPs also demonstrated broad-spectrum antibiofilm activity against test bacteria, ranging from 77.95 to 82.4% inhibition. Microscopic analysis of biofilms showed significant structural change and inhibition. Our results demonstrate appreciable in vitro activity of MO-AgNPs against the selected pathogens, which could be used as an alternative therapeutic agent for treating infection caused by drug-resistant bacteria and preventing biofilm development by bacteria on medical devices and other surfaces.

✉ Iqbal Ahmad
   ahmadiqbal8@yahoo.co.in

1 Department of Agricultural Microbiology, Faculty
   of Agricultural Sciences, Aligarh Muslim University,
   Aligarh 202002, UP, India

Graphical abstract
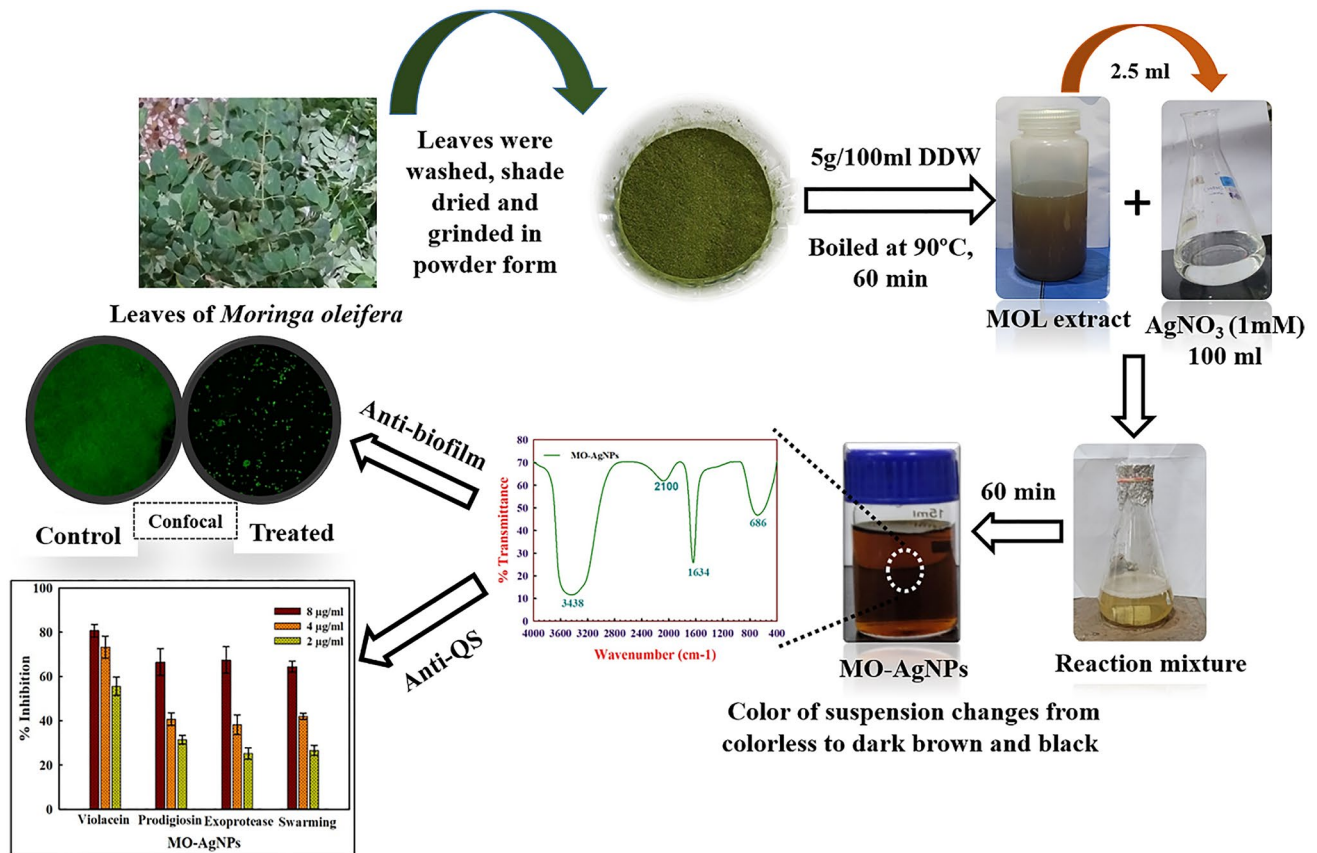
Abbreviations

MO-AgNPs	*Moringa oleifera* mediated synthesis of silver nanoparticles
AMR	Antimicrobial resistance
QS	Quorum sensing
MDR	Multi-drug resistance
XRD	X-ray diffraction
MIC	Minimum inhibitory concentration
TEM	Transmission electron microscopy
FTIR	Fourier-transform infrared spectroscopy
SEM	Scanning electron microscopy
CLSM	Confocal laser scanning microscopy

1 Introduction

Moringa oleifera (Family: Moringaceae) is a widely distributed and quickly proliferating plant, making it an easy source for extracting bioactive components. It has been used in Indian food from the very beginning. The leaves of *Moringa oleifera* are a rich source of proteins (30.3%), amino acids (19), phosphorus (0.3%), potassium (1.5%), calcium (3.0 mg/100g), zinc (13.03 mg/kg), iron (490 mg/kg), vitamin C (18.5mg/100g), and vitamin E (77 mg/100g). It also contains polyphenols (2%), phenolic acids (105.04–308.3 mg GAE/g DW), alkaloids (6.17%), flavonoids (2.5%), tannins (20.7 mg/g), saponins (3.2%), glucosinolates (28.62 μmol/g), 44.4% carbohydrates, β-carotene (161 μg/g), isothiocyanates (1.66%), and oxalates (10.5 mg/g) [1]. These substances can act as stabilizing and reducing agents during the synthesis of silver nanoparticles. It is well-recognized for its several medical benefits, including antibacterial action. As a result, it is an excellent option for synthesizing AgNPs with improved antibacterial characteristics. Powder of Moringa leaves has more calcium than milk. In addition, it contains iron, making it a potential substitute for beet and spinach in the treatment of anemia caused due to deficiency of iron [2]. Due to its low cost and availability, *Moringa oleifera* may be exploited for the green synthesis of nanoparticles. However, little information is available on this plant [3]

Antimicrobial resistance (AMR) has emerged as a global threat to the current healthcare system that might impede the control of many infectious illnesses and significantly regress modern medicine. The overuse and abuse of antimicrobials in medical and non-medical settings have exacerbated the global epidemic of AMR since the discovery of the first antibiotics that consistently benefitted human medicine. Due to the risk of the emergence of resistance, even novel antimicrobials that aim to inhibit bacterial growth cannot be trusted for sustained administration. Antimicrobials with new modes of action against MDR pathogens are still in the early stages of development [4] and are being actively influenced by research in the realm of nanotechnology. By reducing the material to a nanoscale, the characteristics can be enhanced, improving function [5]. The physical and chemical strategies for nanoparticle synthesis might result in unforeseen consequences like high energy use and environmental contamination [6]. The "green synthesis" approaches/methods are receiving much interest in the present research because they decrease waste generation, reduce pollution, and employ cleaner, renewable auxiliary materials. Hence, the green production of nanoparticles is likewise rated as an environmentally benign method [4]. It has been determined that the green synthesis of nanoparticles, which uses plant extracts and microorganisms for synthesis, is a more environmentally friendly method for synthesizing AgNPs. Polyphenols, proteins, amides, phenolic acids, terpenoids, and ketones are examples of plant phytochemicals or secondary metabolites that continuously play a crucial role in the creation of nanoparticles [7]. Many researchers describe the production of AgNPs with substantial antibacterial activity using plant extracts: *Murraya koenigii* (curry leaf)[8], *Xanthium strumerium* L. [9], *Macrotyloma uniflorum* [10], root extracts of *Trianthema decandra* [11]. The antibacterial efficacy and stability of AgNPs is dependent on the propensity to form aggregates and the ability of releasing silver ions [12]. AgNPs coated with *Agrimoniae herba* extract demonstrated both as reducing and stabilizing agents, which enhanced therapeutic efficacy [13]. The primary metabolites found in plant extracts, such as reducing sugar, proteins, peptides, amino acids, etc., are crucial for the reduction and stabilization of metallic silver into AgNPs. The synthesis of stable AgNPs is brought about by flavonoids and terpenoids found in the leaf extract of *A. indica* [14]. Numerous studies revealed that proteins may also serve as stabilizing agents in addition to bioreduction [15]. With the increasing problem of multi-drug resistance in pathogenic bacteria, the efficacy of available antibiotics and other antibacterial agents is continuously decreasing. To combat such pathogenic bacteria, novel anti-infective drug targets such as quorum sensing and biofilms seem to be attractive options. In recent years, green synthesized nanoparticles have demonstrated activity against QS-mediated virulence factors in pathogenic bacteria. However, research data on broad-spectrum green synthesized active nanoparticles with improved efficacy and stability is limited. Therefore, we hypothesized that green synthesis of silver nanoparticles using bioactive plant extract might result in the development of silver nanoparticles with improved efficacy and stability against bacterial pathogens. Hence, this work used *Moringa oleifera* leaf extract (MOL) to synthesize AgNPs.

2 Material and methods

2.1 Chemicals and reagents

Azocasein and Triphenyl tetrazolium chloride (TTC) were purchased from Sigma Aldrich, USA and SRL Pvt. Ltd, respectively. Microbiological media (LB Agar) and orcinol were obtained from Hi-Media, India. All organic solvents, chemicals, and reagents were of analytical grade.

2.2 Synthesis of silver nanoparticles using *Moringa oleifera* leaves extract

Moringa oleifera leaves were collected locally from Aligarh, UP, India. The identity of the plant was confirmed locally by the Botany Department, AMU, Aligarh. After being cleaned of debris and dust, the leaves were dried in the shade for four days. The sample has been submitted to the departmental repository together with the voucher specimen (MZK-MO-19/20).

The *Moringa oleifera* aqueous extract was made by adding 5 g of powdered dry leaves in double distilled water (100 ml). Suspension was then filtered after it had been heated for an hour at 90 °C. 1 mM $AgNO_3$ aqueous solution (100 mL) and 2.5 mL of *Moringa oleifera* aqueous extract were mixed to synthesize MO-AgNPs. In a volumetric flask, $AgNO_3$ was reduced by plant extract while continuously stirred with a magnetic stirrer at room temperature. The change in color of the reaction mixture was recorded as brown, followed by light black, indicating the reduction of $AgNO_3$. The synthesized MO-AgNPs were separated by centrifugation for 30 min at 12,000 rpm, followed by repeated washing and dried at 55 °C overnight [4].

2.3 Characterization of silver nanoparticles

UV–visible spectroscopy was employed to characterize MO-AgNPs at the preliminary level. UV–visible spectra of MO-AgNPs was obtained in a range of wavelength (300–600 nm), followed by X-ray diffraction, FTIR, TEM, and SEM–EDX, as mentioned previously [4]. The spectral measurements were continued for up to 6 months at regular intervals of 15 days to assess the stability of MO-AgNPs.

2.4 Bacterial cultures used

C. violaceum ATCC 12472 (ATCC, USA), *S. marcescens* (isolate, ZH3), and *E. fergusonii* (isolate, Z2) were used in this study. Luria Bertani (LB) broth was used to cultivate all test pathogens.

2.5 Minimum inhibitory concentration of MO-AgNPs against test pathogens

Using the specific dye TTC as a growth indicator, the MIC of MO-AgNPs against bacterial pathogens was calculated by the previously mentioned micro broth dilution technique [16].

2.6 Violacein production

The previously described standard methodology [17] was used to qualitatively evaluate the violacein inhibitory action of MO-AgNPs. Five millilitres of LB soft agar (0.5% w/v agar) containing *C. violaceum* 12,472 was overlaid on LB agar plates, and let the plates were kept standing for twenty minutes. Sterile discs (8 mm) impregnated with varying concentrations of the MO-AgNPs were mounted on the solid media. For 24 h, plates were left incubated at 30°C, and the pigment inhibition in the form of a halo zone around the discs was recorded. Growth inhibition, in the form of clear zones around the impregnated disc, if present, was also monitored. The results were expressed in diameter (mm) of pigment inhibition or growth inhibition.

Violacein quantification in treated and untreated culture with MO-AgNPs at sub-MICs (0.5–8 µg/mL) was determined using a previously reported procedure [18].

2.7 Assays for production of QS-controlled virulence factors in *S. marcescens*

2.7.1 Production of prodigiosin

In Luria–Bertani media, prodigiosin pigment was evaluated using the established procedure as mentioned previously [19]. Briefly, at sub-MICs of the test agent, the bacterial culture was grown for 18 h at 30 °C. The bacterial cells were pelleted by centrifuging two millilitres of the growing culture at 10,000 rpm for five minutes. A rigorous vortexing process lasting 5 min was used to dissolve the pellet in 1 ml of an acidified ethanol solution. In order to eliminate debris, the sample was centrifuged once more for five minutes at a speed of 13,000 rpm. Using a UV-2600 spectrophotometer, the absorbance was measured at 534 nm.

2.7.2 Exoprotease activity

As stated before, the azocasein degradation method was used to assess the exoprotease activity of *Serratia marcescens* [20]. In brief, *Serratia marcescens* was cultivated for 18 h at 30 °C at sub-MICs of MO-AgNPs. The parallel control set was run without MO-AgNPs. 1 millilitre azocasein (0.3% w/v) was combined with a hundred microlitres of the supernatant obtained after centrifuging the culture. 15 min of shaking-induced incubation at 37°C was performed on the reaction mixture. Centrifugation was used to eliminate the undissolved azocasein after the process was halted by introducing 0.5 millilitres of ice-cold TCA. Using a UV-2600 spectrophotometer, the absorbance was measured at 400 nm.

2.7.3 Motility assay

In order to assess the swarming motility, MO-AgNPs amended LB plates (0.5% agar) were spotted with 5 µl of the freshly grown bacterial culture. The control group consisted of plates devoid of MO-AgNPs. After 18 h of incubation, the bacterial swarm diameter was measured in mm.

2.8 Biofilm inhibition assay

2.8.1 Crystal violet method

By employing the previously reported crystal violet method using a microtitre plate (96 wells), MO-AgNPs' quantitative evaluation of biofilm inhibition was assessed [21]. Bacterial cultures with different sub-MICs of MO-AgNPs were introduced to the wells containing LB medium, followed by overnight incubation. Wells were cleaned three times with autoclaved PBS to eliminate excess broth and planktonic cells, and then they were allowed to air dry for 20 min. After 15 s of staining with 200 µl crystal violet, the biofilms were gently washed three times to remove the stain. 200 µl of 90% ethanol was used to extract the crystal violet attached to the biofilm, and with the use of a microplate reader, the absorbance was measured at 620 nm.

2.8.2 Visualization of biofilm by light microscopy

The previously reported approach was used to inhibit biofilms on glass coverslips [22]. In brief, a 24-well culture plate with 3 ml of culture medium was seeded with 60 µl overnight developed cultures of the test microorganisms. Additionally, the wells received sterile glass coverslips with the corresponding highest sub-MICs of MO-AgNPs. Following a 24-h incubation period, the loosely attached cells were washed 3 times with sterile phosphate buffer solution and then allowed to air dry for twenty minutes. After staining with crystal violet solution, slides were allowed to air

dry for 30 min. A light microscope (Olympus BX60, Model BX60F5, Olympus Optical Co., Ltd., Japan) with a color VGA camera (Sony, Model no. SSC-DC-58AP, Japan) was used to view the biofilms.

2.8.3 Microscopic examination of biofilms by SEM and CLSM

As previously indicated, biofilms developed on coverslips. Following washing with autoclaved PBS and fixing with 2.5% glutaraldehyde, unbound bacterial cells were eliminated. After that, a gradient of ethanol was used to dry the adhering cells and biofilms for ten minutes. Before visualization, the slides were gold-coated and allowed to air dry. The USIF, AMU, Aligarh used a JEOL-JSM 6510 LV to capture the SEM micrographs.

The same process described above was used for Confocal Laser Scanning Microscopy to grow biofilms on glass surfaces, after which acridine orange (0.1%) was used to stain the biofilms for 20 min. At USIF, AMU, Aligarh, the photos were captured using a Zeiss LSM780.

2.9 Statistical analysis

Three replicates of each experiment were conducted. Each experiment was repeated at least two times. The control and treatment groups were compared using the t test. P values ≤ 0.05 were considered significant.

3 Results

3.1 Characteristics of MO-AgNPs

In this work, the aqueous extract of *Moringa oleifera* was used to synthesize the silver nanoparticles (Supplementary Fig. S1). The change in color of the silver nitrate solution went from being colorless to dark brown and black. Silver nanoparticles produced in the reaction medium exhibit an absorption band near 440 nm (Fig. 1), which is associated with spherical-shaped silver nanoparticles. The stability was observed by recording absorbance spectra, which did not alter after storage at room temperature for six months (Supplementary Fig. S2).

The crystal structure and particle size of MO-AgNPs were determined using the XRD method. Figure 2 shows the XRD pattern, with four prominent peaks in the spectrum of 2θ values ranging from 20 to 80. The diffractions at 38.06°, 44.28°, 64.64° and 77.44° can be indexed to the [111], [200], [220], and [311] planes of the face-centered cubic (fcc) silver, respectively, indicating the crystalline nature of MO-AgNPs (JCPDS file No. 04–0783). Additional peaks are seen in addition to the silver nanoparticle peaks, indicating the
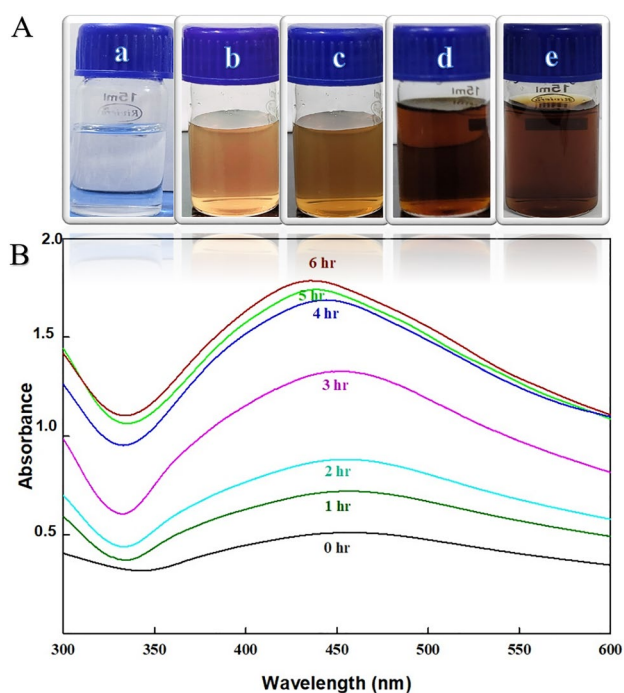
Fig. 1 (**A**) Observation of the color change caused by produced silver nanoparticles representing **a** aqueous AgNO$_3$ solution, **b–e** MO-AgNPs at 0 h, 1h, 2 h, and 3 h respectively (**B**) UV–visible spectra of MO-AgNPs
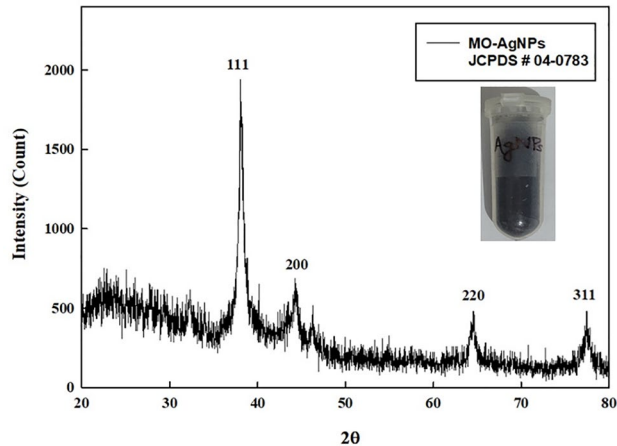

Fig. 2 XRD pattern of MO-AgNPs

existence of organic materials linked to MO-AgNPs. Using the Debye–Scherrer formula, the particle size averaged to be 26.19 nm.

Figure 3A depicts a TEM image of MO-AgNPs. The nanoparticles have a range of sizes, as seen by micrographs. Further, SEM verified the morphology of MO-AgNPs. Most of the particles were spherical in form (Fig. 3B-i). Capping of MO-AgNPs with phytoconstituents can be seen, which

Fig. 3 (**A**) Transmission electron micrograph of synthesized MO-AgNPs. (**B**) Analyses of MO-AgNPs by SEM and EDX. Panel (**B-i**) depicts the SEM micrograph of MO-AgNPs; Panel (**B-ii**) depicts the EDX spectra of MO-AgNPs; Panel (**B-iii**) represents the weight % histogram of the main constituents in MO-AgNPs
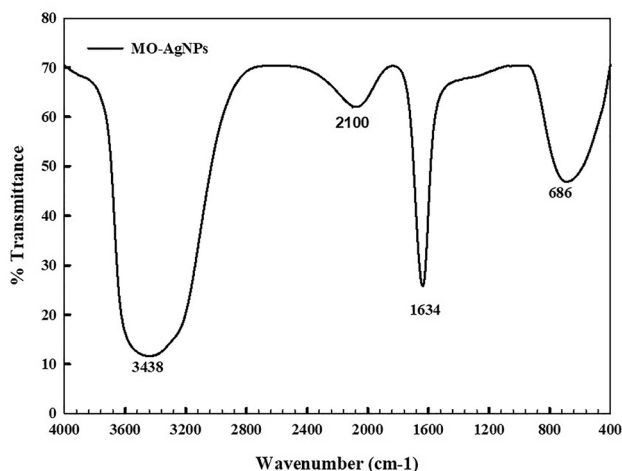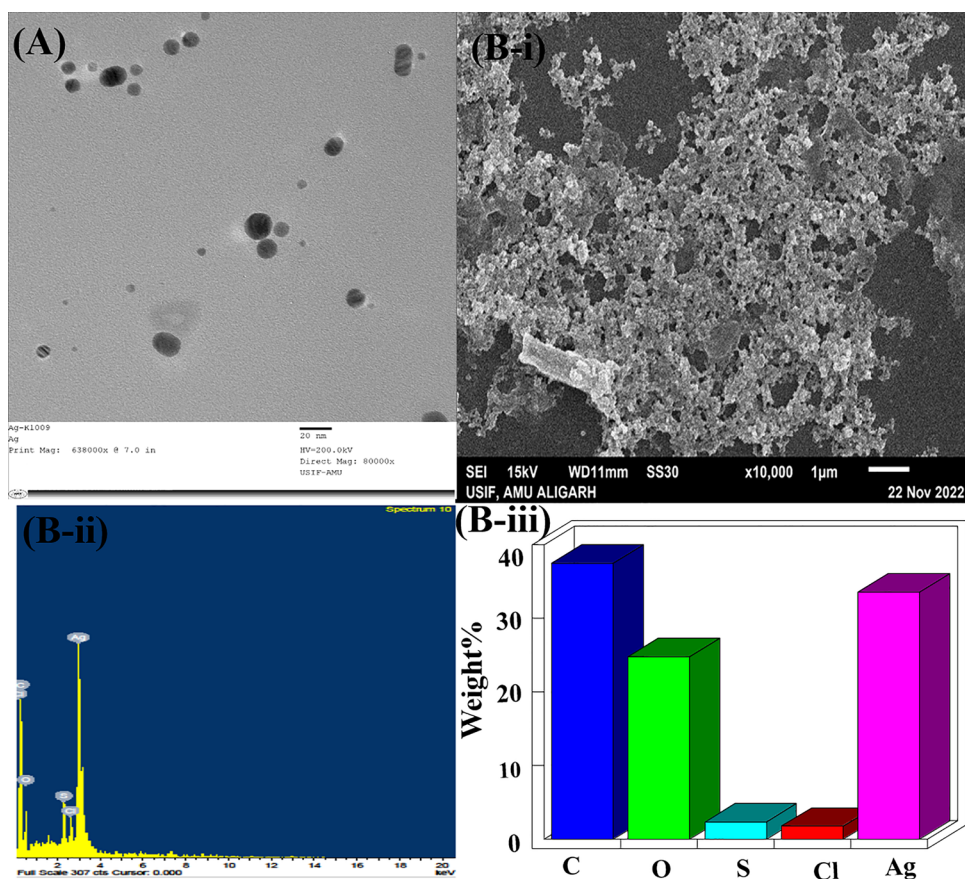
Fig. 4 FTIR spectrum of MO-AgNPs

imparts greater stability. The EDX spectrum used to examine the elemental composition of MO-AgNPs is shown in Fig. 3B-ii, where along with signals for the components C, O, S, and Cl, a silver signal (33.55%) indicated the existence of elemental silver in the reaction medium.

The FTIR spectrum of MO-AgNPs is shown in Fig. 4. MO-AgNPs have 4 strong FTIR spectral transmittance

troughs at 680 cm^{-1}, 1638 cm^{-1}, 2100 cm^{-1}, and 3436 cm^{-1} region, respectively.

3.2 MIC of MO-AgNPs

The minimum inhibitory concentration of MO-AgNPs against *Chromobacterium violaceum* 12,472, *Escherichia fergusonii,* and *Serratia marcescens* was found to be 16, 16, and 32 µg/ml, respectively. All experiments on inhibition of QS and biofilms was performed using respective sub-MICs against test bacteria.

3.3 Effect of MO-AgNPs on violacein production

MO-AgNPs were primarily assessed against the production of violacein by CV 12472 by disc diffusion method at 4 µg/ml/disc and 8 µg/ml/disc concentrations. MO-AgNPs exhibited varying levels of pigment inhibition at tested concentrations (Fig. 5A).

The quantitative estimation of violacein inhibition was done at varying levels of sub-MICs (0.5–8 µg/ml) of MO-AgNPs. The ability of MO-AgNPs to reduce violacein production was measured spectrophotometrically. At 0.5, 1, 2, and 4 µg/ml, 27.4, 36.4, 55.5, and 73.2% inhibition of violacein production was recorded as compared to control
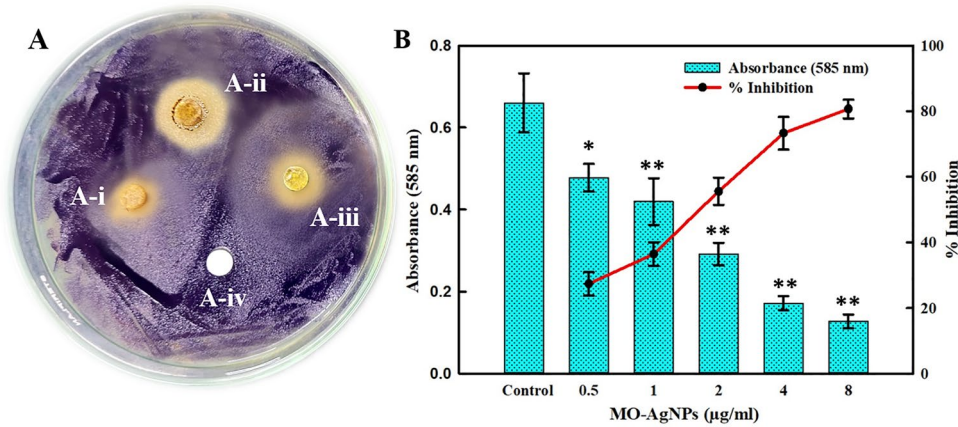
Fig. 5 (**A**) Effect of MO-AgNPs on the production of violacein by CV 12472 by disc diffusion. **A-i**: MO-AgNPs (4 μg/ml); **A-ii**: MO-AgNPs (8 μg/ml); **A-iii**: *M. oleifera* (Aqueous: 1 mg/ml); A-iv: DMSO (control). (**B**) Analysis of violacein reduction in CV 12472 quantitatively at different sub-MICs of MO-AgNPs. Data are shown as the average of three readings, with SD shown by the bar. The secondary y-axis displays the % inhibition. $P \leq 0.05$ and $P \leq 0.005$ are indicated by symbols * and **, respectively

(Fig. 5B). Pigment production was seen to be inhibited by 80.6% at ½ × MIC (8 μg/ml).

3.4 Effect of MO-AgNPs on virulence factors of *Serratia marcescens*

With increasing concentration of MO-AgNPs, prodigiosin pigment synthesis was seen to decrease in a concentration-dependent manner. Prodigiosin production was reduced by 31.4, 40.6, 66.5 and 77.4% following treatment with 2, 4, 8, and 16 μg/ml of MO-AgNPs, respectively (Fig. 6A). The proteolytic activity of MO-AgNPs was also evaluated in *S. marcescens* to determine their broad-spectrum anti-QS action. *S. marcescens* has exoproteinases as its primary source of proteolytic activity. A concentration-dependent response to exoprotease activity was clearly shown by the findings of our study (Fig. 6B). Exoprotease activity was inhibited by 25.1, 38.1, 67.4, and 76.02%, at concentrations of 2, 4, 8, and 16 μg/ml of MO-AgNPs, respectively. To the best of our knowledge, the anti-QS effect of MO-AgNPs in *S. marcescens* has not been reported previously.

Fig.6 (**A**) Effect of MO-AgNPs on production of prodigiosin in *Serratia marcescens*. (**B**) Effect of MO-AgNPs on production of exoprotease in *S. marcescens*. Data are shown as the average of three readings, with SD shown by the bar. $P \leq 0.005$ is indicated by the symbol **. (**C**) Sub-MIC levels of MO-AgNPs inhibit *S. marcescens*' ability to swim (i) Control; (ii) 4 μg/ml; (iii) 8 μg/ml; (iv) 16 μg/ml MO-AgNPs
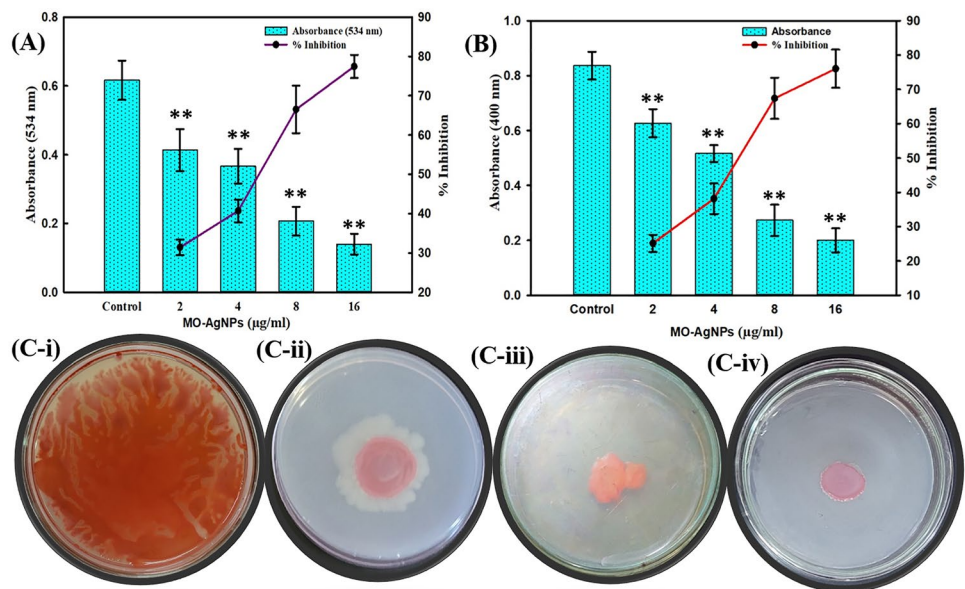
MO-AgNPs were further tested for their ability to prevent *S. marcescens* from swarming over agar plates. Within 18 h of incubation, the untreated control of *S. marcescens* swarmed through the whole plate with 89 mm zone diameter (Fig. 6C). After being treated with 2, 4, and 8 µg/ml of MO-AgNPs, the swarming motility was reduced by 26.5, 41.9, and 64.4% respectively. The swarming motility was decreased by 86.5% at the highest level of sub-MIC (16 µg/ml) used.

Table 1 Effect of Sub-MICs of MO-AgNPs on biofilm formation by different pathogenic bacterial strains

Fraction con-centration	OD_{620nm}		
	S. marcescens	*E. fergusonii*	*C. violaceum*
Control	0.89 ± 0.06	0.71 ± 0.04	0.80 ± 0.07
1 µg/ml	$0.79 \pm 0.03*$ (10.72)	$0.56 \pm 0.04*$ (20.17)	$0.51 \pm 0.02*$ (36.55)
2 µg/ml	$0.72 \pm 0.06**$ (18.42)	$0.52 \pm 0.06**$ (26.95)	$0.44 \pm 0.06**$ (45.08)
4 µg/ml	$0.51 \pm 0.03*$ (42.02)	$0.4 \pm 0.05**$ (43.38)	$0.28 \pm 0.05**$ (65.21)
8 µg/ml	$0.32 \pm 0.04**$ (63.41)	$0.15 \pm 0.03**$ (77.95)	$0.14 \pm 0.05**$ (82.40)
16 µg/ml	$0.16 \pm 0.02**$ (81.5)	NT	NT

OD_{620} is used to measure biofilm development following crystal violet incubation

The data is the average value from three separate experiments. $P \leq 0.05$ and $P \leq 0.005$ are indicated by symbols * and **, respectively. *NT* represents Not Tested

The percent decrease over control is shown by the value in parentheses

3.5 Effect of MO-AgNPs on bacterial biofilm development

The suppression of biofilm production by MO-AgNPs against test bacteria is shown in Table 1. In the presence of 1, 2, 4, 8, and 16 µg/ml MO-AgNPs, the biofilms of *Serratia marcescens* were reduced by 10.7, 18.4, 42, 63.4, and 81.5% respectively. Similarly, treatment with 1, 2, 4, and 8 µg/ml MO-AgNPs resulted in biofilm suppression by *C. violaceum* by 36.5, 45, 65.2, and 82.4% respectively. The biofilms of *Escherichia fergusonii* were suppressed by 20.1, 26.9, and 43.3% on supplementation of 1, 2, and 4 µg/ml MO-AgNPs, respectively, in growth media. There was 77.9% suppression of biofilm relative to untreated control at the highest level of sub-MIC used (8 µg/ml).

Microscopic analysis on glass coverslips was used to further evaluate the quantitative results of reduction in biofilm formation acquired by microtitre plate assay. Untreated bacterial cells produced thick, mat-like materials on the surface of the glass, as shown by the light microscopic image (supplementary Fig. S3). Cell adhesion to the glass surface was decreased after treatment with respective ½ × MICs. The treated cells are organized into small microcolonies with less biofilms. SEM images further showed the biofilm inhibition by MO-AgNPs with scattered cells in comparison to the untreated control (Fig. 7). The above findings were also validated by the CLSM study. In the presence of MO-AgNPs, the group of cells that had grown on glass coverslips was extensively diminished (Fig. 8).

4 Discussion

The noticeable change in the color of the AgNO₃ solution from colorless to dark brown and black demonstrates the production of AgNPs [23]. A band of absorption around

Fig. 7 SEM images of *E. fergusonii*, *C. violaceum, and S. marcescens* biofilm in the absence and presence of sub-MICs of MO-AgNPs

Fig. 8 CLSM images of *E. fergusonii*, *C. violaceum,* and *S. marcescens* biofilm in the absence and presence of sub-MICs of MO-AgNPs
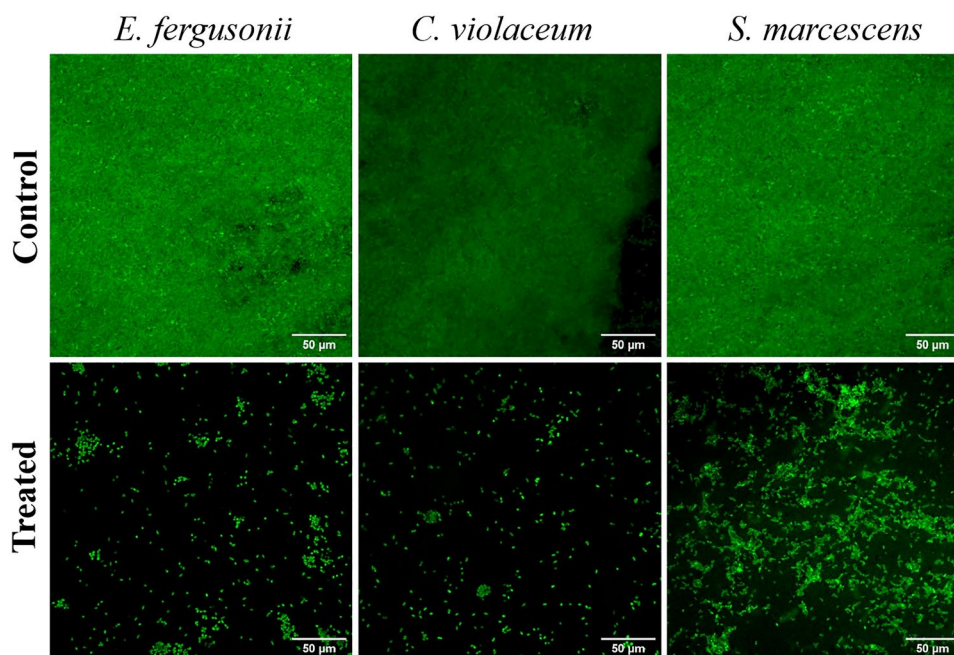
440 nm was visible in the absorption spectra of silver nanoparticles produced in the reaction medium, which is associated with spherical AgNPs and ascribed to the SPR band of MO-AgNPs[24]. The biological process is employed to create nanoparticles by the bio-genic synthesis from plants and their derivatives. Plant extracts that contain bioactive components such as alkaloids and phenolic compounds demonstrate bioreduction capabilities and function as stabilizing and reducing agents [25].

Proteins, alkaloids, flavonoids, tannins, carbohydrates, triterpenoids, and metabolites are found in *Moringa oleifera* leaf extract, which could serve as a stabilizing agent, thereby preventing electrostatic aggregation of the nanoparticles [1]. Using the XRD method, the particle size averaged to be 26.19 nm. It has been shown that *Mentha Piperita*, *Azadirachta indica*, *Pelargonium graveolens*, and *Eucalyptus hybrida* leaf extracts may be used to synthesize AgNPs in size ranges of 5–30, 25–40, 50–100, 16–40, and 15–150 nm respectively [26]. Additional peaks were seen in addition to the silver nanoparticle peaks, indicating the existence of organic materials linked to MO-AgNPs. This result is consistent with the findings of the study [27]. The nanoparticles have a range of sizes, as seen by the TEM image. The particles were mostly spherical, as seen by the SEM image. The EDX spectrum showed a silver signal (33.55%) along with signals for the components C, O, S, and Cl. The biomolecules attached to the surface of the silver nanoparticles may be the cause of the weak signal[26]. In order to understand how different functional groups of *Moringa oleifera* phytoconstituents contributed to the production and stabilization of MO-AgNPs, FTIR analysis was done. The FTIR spectrum of MO-AgNPs showed 4 strong FTIR spectral transmittance troughs at 680 cm^{-1}, 1638 cm^{-1}, 2100 cm^{-1}, and 3436 cm^{-1} region, respectively. The peaks that arise between 600–1400 belong to the C-O- carboxyl groups or the C-N group, reflecting the amount of proteins in plant leaves[28]. Further, the peaks at 1638, 2100, and 3436 belong to C=O carbonyl stretching, –C≡C– stretch, and the presence of the O–H bond of phenolic compounds, respectively. In addition to acting as a stabilizing factor and possibly hindering aggregation of nanoparticles by linking to AgNPs via free amino groups or cysteine residues, the presence of proteins and phenols acts as a reducing factor. The AgNPs synthesized using *Moringa oleifera* (Leaves extract) demonstrated antibacterial activity against pathogenic *Klebsiella pneumoniae*, *Staphylococcus aureus*, *Bacillus cereus, E.coli,* and *Candida tropicalis* [3]. Violacein production was seen to be inhibited by 80.6% at ½×MIC (8 μg/ml). In previous findings, silver nanoparticles made from *Crataeva nurvala* reduced violacein synthesis on agar plates at a concentration of 15 μg/ml [29]. Prodigiosin is a red-pigmented secondary product in *S. marcescens* whose production is regulated by Quorum sensing [30]. With increasing concentration of MO-AgNPs, prodigiosin pigment synthesis was seen to decrease in a concentration-dependent manner. Earlier, *Anethum graveolens* extract at 512 μg/ml inhibited prodigiosin pigment by 66% with respect to control [20]. A concentration-dependent response to exoprotease activity was clearly shown by the findings of our study. *Serratia marcescens* has exoproteinases as its primary source of proteolytic activity. One of the primary pathogenic characteristics of *S. marcescens* is thought to be exoproteases [31]. Virulent strains of *S. marcescens* are

distinguished by their high motility, which also contributes to some hospital-acquired infections [20]. *Serratia marcescens* adheres to solid surfaces with the help of the motilities mediated by flagella, which promote the formation of biofilms [32]. Bacterial biofilms are bacterial populations that adhere to surfaces bound by their self-secreted matrix of polymeric substances, including polysaccharides, secreted proteins, and extracellular DNAs. The biofilms of *Escherichia fergusonii, Serratia marcescens,* and *Chromobacterium violaceum* showed concentration-dependent inhibition with increasing concentrations of MO-AgNPs. Earlier, biofilms formed by *S. aureus* and *P. aeruginosa* showed concentration-dependent inhibition with increasing concentrations of ELE-AgNPs [26]. Also, biofilms formed by various gram-positive and gram-negative bacteria were found to be inhibited with increasing concentrations of Alb-AgNPs [33]. The importance of biofilms in medical science is due to their significance in bacterial pathogenesis and the difficulties in eliminating them with antibiotics [34]. Bacteria coordinate the expression of their genes as they develop in biofilms, increasing their resistance to therapeutic agents that are both chemical and physical [35]. A previous study revealed that *P. aeruginosa* in biofilms had a 1000-fold increase in tobramycin resistance compared to their planktonic counterparts [36]. It has been shown that nanoparticles may attach to and permeate bacterial membranes, build up inside bacterial cells, and destroy bacterial cells [37].

5 Conclusion

The finding concludes that *Moringa oleifera* mediated synthesis of silver nanoparticles (MO-AgNPs) were spherical in shape with an average particle size of 26.19 nm, showing capping with phytoconstituents and enhanced stability at room temperature. The MO-AgNPs demonstrated broad-spectrum anti-QS and anti-biofilm efficacy against bacterial pathogens, indicating their therapeutic potential. The ability of Ag$^+$ ions to permeate the bacterial biofilm matrix accounts for the antibiofilm mechanism of action of MO-AgNPs. Both SEM and confocal microscopic analysis revealed disruptions in biofilm establishment on abiotic surfaces. Therefore, MO-AgNPs might also be used as surface-coating agents to prevent bacterial adhesion and bacterial infections associated with medical implants. Further, in vivo efficacy of MO-AgNPs is to be evaluated to assess the safety of *Moringa oleifera*-synthesized AgNPs. Also, the potential synergistic effects of AgNPs is to be investigated with other antimicrobial agents, such as natural compounds.

Supplementary Information The online version contains supplementary material available at https://doi.org/10.1007/s43994-023-00089-8.

Declarations

Conflict of interest The authors declare that there is no conflict of interest.

References

1. Stohs SJ, Hartman MJ (2015) Review of the safety and efficacy of moringa oleifera. Phytother Res 29:796–804. https://doi.org/10.1002/ptr.5325

2. Patil SV, Mohite BV, Marathe KR, Salunkhe NS, Marathe V, Patil VS (2022) Moringa tree, gift of nature: a review on nutritional and industrial potential. Curr Pharmacol Rep 8:262–280. https://doi.org/10.1007/s40495-022-00288-7

3. Prasad T, Elumalai EK (2011) Biofabrication of Ag nanoparticles using Moringa oleifera leaf extract and their antimicrobial activity. Asian Pac J Trop Biomed 1:439. https://doi.org/10.1016/S2221-1691(11)60096-8

4. Qais FA, Shafiq A, Ahmad I, Husain FM, Khan RA, Hassan I (2020) Green synthesis of silver nanoparticles using *Carum copticum*: assessment of its quorum sensing and biofilm inhibitory potential against gram-negative bacterial pathogens. Microb Pathog 144:104172. https://doi.org/10.1016/j.micpath.2020.104172

5. Bindhu MR, Umadevi M, Esmail GA, Al-Dhabi NA, Arasu MV (2020) Green synthesis and characterization of silver nanoparticles from Moringa oleifera flower and assessment of antimicrobial and sensing properties. J Photochem Photobiol B 205:111836. https://doi.org/10.1016/j.jphotobiol.2020.111836

6. Gupta R, Xie H (2018) Nanoparticles in daily life: applications, toxicity and regulations. J Environ Pathol Toxicol Oncol 37:209–230. https://doi.org/10.1615/JEnvironPatholToxicolOncol.2018026009

7. Salayová A, Bedlovičová Z, Daneu N, Baláž M, Lukáčová Bujňáková Z, Balážová Ľ et al (2021) Green synthesis of silver nanoparticles with antibacterial activity using various medicinal plant extracts: morphology and antibacterial efficacy. Nanomaterials 11:1005. https://doi.org/10.3390/nano11041005

8. Christensen L, Vivekanandhan S, Misra M, Kumar MA (2011) Biosynthesis of silver nanoparticles using *Murraya koenigii* (curry leaf): an investigation on the effect of broth concentration in reduction mechanism and particle size. Adv Mater Lett 2:429–434. https://doi.org/10.5185/amlett.2011.4256

9. Mittal J, Jain R, Sharma MM (2017) Phytofabrication of silver nanoparticles using aqueous leaf extract of *Xanthium strumerium* L. and their bactericidal efficacy. Adv Nat Sci: Nanosci Nanotechnol 8:025011. https://doi.org/10.1088/2043-6254/aa6879

10. Vidhu VK, Aromal SA, Philip D (2011) Green synthesis of silver nanoparticles using *Macrotyloma uniflorum*. Spectrochim Acta Part A Mol Biomol Spectrosc 83:392–397. https://doi.org/10.1016/j.saa.2011.08.051

11. Geethalakshmi R, Sarada DVL (2012) Gold and silver nanoparticles from *Trianthema decandra*: synthesis, characterization, and antimicrobial properties. Int J Nanomed 7:5375. https://doi.org/10.2147/IJN.S36516

12. Panacek A, Kvítek L, Prucek R, Kolar M, Vecerova R, Pizúrova N et al (2006) Silver colloid nanoparticles: synthesis, characterization, and their antibacterial activity. J Phys Chem B 110:16248–16253. https://doi.org/10.1021/jp063826h

13. Qu D, Sun W, Chen Y, Zhou J, Liu C (2014) Synthesis and in vitro antineoplastic evaluation of silver nanoparticles mediated by *Agrimoniae herba* extract. IJN 9:1871–1882. https://doi.org/10.2147/IJN.S58732

14. Shankar SS, Rai A, Ahmad A, Sastry M (2004) Rapid synthesis of Au, Ag, and bimetallic Au core–Ag shell nanoparticles using Neem (*Azadirachta indica*) leaf broth. J Colloid Interface Sci 275:496–502. https://doi.org/10.1016/j.jcis.2004.03.003

15. Reddy M, Sri Rama Murthy K, Srilakshmi A, Sambasiva Rao KRS, Pullaiah T (2015) Phytosynthesis of eco-friendly silver nanoparticles and biological applications—a novel concept in nanobiotechnology. Afr J Biotechnol 14:222–47. https://doi.org/10.5897/AJB2013.13299

16. Eloff JN (1998) A sensitive and quick microplate method to determine the minimal inhibitory concentration of plant extracts for bacteria. Planta Med 64:711–713. https://doi.org/10.1055/s-2006-957563

17. McLean RJC, Pierson LS, Fuqua C (2004) A simple screening protocol for the identification of quorum signal antagonists. J Microbiol Methods 58:351–360. https://doi.org/10.1016/j.mimet.2004.04.016

18. Matz C, Deines P, Boenigk J, Arndt H, Eberl L, Kjelleberg S et al (2004) Impact of violacein-producing bacteria on survival and feeding of bacterivorous nanoflagellates. Appl Environ Microbiol 70:1593–1599. https://doi.org/10.1128/AEM.70.3.1593-1599.2004

19. Slater H, Crow M, Everson L, Salmond GPC (2003) Phosphate availability regulates biosynthesis of two antibiotics, prodigiosin and carbapenem, in Serratia via both quorum-sensing-dependent and -independent pathways. Mol Microbiol 47:303–320. https://doi.org/10.1046/j.1365-2958.2003.03295.x

20. Salini R, Pandian SK (2015) Interference of quorum sensing in urinary pathogen Serratia marcescens by *Anethum graveolens*. Pathog Dis 73:ftv08. https://doi.org/10.1093/femspd/ftv038

21. O'Toole GA, Kolter R (1998) Flagellar and twitching motility are necessary for *Pseudomonas aeruginosa* biofilm development. Mol Microbiol 30:295–304. https://doi.org/10.1046/j.1365-2958.1998.01062.x

22. Sybiya Vasantha Packiavathy IA, Agilandeswari P, Musthafa KS, Karutha Pandian S, Veera Ravi A (2012) Antibiofilm and quorum sensing inhibitory potential of *Cuminum cyminum* and its secondary metabolite methyl eugenol against Gram negative bacterial pathogen. Food Res Int 45:85–92. https://doi.org/10.1016/j.foodres.2011.10.022

23. Gurunathan S, Kalishwaralal K, Vaidyanathan R, Venkataraman D, Pandian SRK, Muniyandi J et al (2009) Biosynthesis, purification and characterization of silver nanoparticles using *Escherichia coli*. Coll Surf B Biointerfaces 74:328–335. https://doi.org/10.1016/j.colsurfb.2009.07.048

24. Rai M, Ingle AP, Gade A, Duran N (2015) Synthesis of silver nanoparticles by Phoma gardeniae and in vitro evaluation of their efficacy against human disease-causing bacteria and fungi. IET Nanobiotechnol 9:71–75. https://doi.org/10.1049/iet-nbt.2014.0013

25. Yadav A, Jangid N, Khan A (2023) Biogenic synthesis of ZnO nanoparticles from *Evolvulus alsinoides* plant extract. J Umm Al-Qura Univ Appl Sci. https://doi.org/10.1007/s43994-023-00076-z

26. Ali K, Ahmed B, Dwivedi S, Saquib Q, Al-Khedhairy A, Musarrat J (2015) Microwave accelerated green synthesis of stable silver nanoparticles with *Eucalyptus globulus* leaf extract and their antibacterial and antibiofilm activity on clinical isolates. PLoS One. https://doi.org/10.1155/2022/4136641

27. Mohammed GM, Hawar SN (2022) Green biosynthesis of silver nanoparticles from *Moringa oleifera* leaves and its antimicrobial and cytotoxicity activities. Int J Biomate. https://doi.org/10.1155/2022/4136641

28. Sampaio S (2018) Production of silver nanoparticles by green synthesis using artichoke (*Cynara scolymus* L.) aqueous extract and measurement of their electrical conductivity. Adv Natural Sci Nanosci Nanotechnol. https://doi.org/10.1088/2043-6254/aae987

29. Ali SG, Ansari MA, Khan HM, Jalal M, Mahdi AA, Cameotra SS (2017) Crataeva nurvala nanoparticles inhibit virulence factors and biofilm formation in clinical isolates of *Pseudomonas aeruginosa*. J Basic Microbiol 57:193–203. https://doi.org/10.1002/jobm.201600175

30. Sakuraoka R, Suzuki T, Morohoshi T (2019) Distribution and genetic diversity of genes involved in quorum sensing and prodigiosin biosynthesis in the complete genome sequences of serratia marcescens. Genome Biol Evol 11:931. https://doi.org/10.1093/gbe/evz046

31. Qais FA, Ahmad I, Altaf M, Manoharadas S, Al-Rayes BF, Abuhasil MSA et al (2021) Biofabricated silver nanoparticles exhibit broad-spectrum antibiofilm and antiquorum sensing activity against Gram-negative bacteria. RSC Adv 11:13700. https://doi.org/10.1039/d1ra00488c

32. Alagely A, Krediet CJ, Ritchie KB, Teplitski M (2011) Signaling-mediated cross-talk modulates swarming and biofilm formation in a coral pathogen Serratia marcescens. ISME J 5:1609. https://doi.org/10.1038/ismej.2011.45

33. Ankudze B, Neglo D (2023) Green synthesis of silver nanoparticles from peel extract of Chrysophyllum albidum fruit and their antimicrobial synergistic potentials and biofilm inhibition properties. Biometals 36:865–876. https://doi.org/10.1007/s10534-022-00483-5

34. Hall CW, Mah T-F (2017) Molecular mechanisms of biofilm-based antibiotic resistance and tolerance in pathogenic bacteria. FEMS Microbiol Rev 41:276–301. https://doi.org/10.1093/femsre/fux010

35. Pompilio A, Crocetta V, Nicola SD, Verginelli F, Fiscarelli E, Bonaventura GD (2015) Cooperative pathogenicity in cystic fibrosis: *Stenotrophomonas maltophilia* modulates *Pseudomonas aeruginosa* virulence in mixed biofilm. Front Microbiol. https://doi.org/10.3389/fmicb.2015.00951

36. Nickel JC, Ruseska I, Wright JB, Costerton JW (1985) Tobramycin resistance of *Pseudomonas aeruginosa* cells growing as a

biofilm on urinary catheter material. Antimicrob Agents Chemother 27:619. https://doi.org/10.1128/aac.27.4.619

37. Mohammad Azam A, Haris Manzoor K, Aijaz Ahmed K, Swaranjit Singh C, Quaiser S, Javed M (2014) Gum arabic capped-silver nanoparticles inhibit biofilm formation by multi-drug resistant strains of *Pseudomonas aeruginosa*. J Basic Microbiol. https://doi.org/10.1002/jobm.201300748